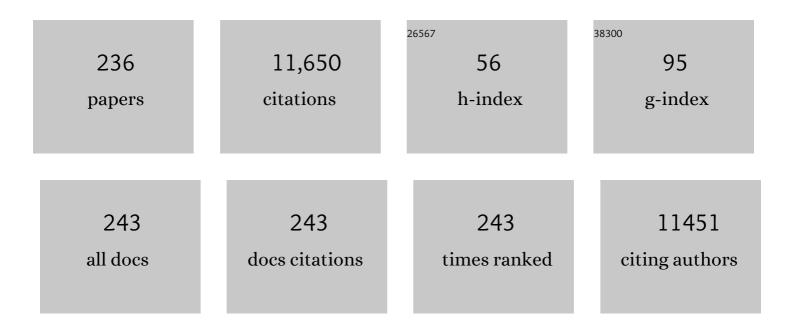
List of Publications by Year in descending order

Source: https://exaly.com/author-pdf/5378990/publications.pdf Version: 2024-02-01



#	Article	IF	CITATIONS
1	Versatile ternary organic solar cells: a critical review. Energy and Environmental Science, 2016, 9, 281-322.	15.6	585
2	Dithieno[3,2â€ <i>b</i> :2′,3′â€ <i>d</i>]pyrrol Fused Nonfullerene Acceptors Enabling Over 13% Efficiency Organic Solar Cells. Advanced Materials, 2018, 30, e1707150.	for 11.1	373
3	Recent progress in the design of narrow bandgap conjugated polymers for high-efficiency organic solar cells. Progress in Polymer Science, 2012, 37, 1292-1331.	11.8	248
4	Toward ideal hole transport materials: a review on recent progress in dopant-free hole transport materials for fabricating efficient and stable perovskite solar cells. Energy and Environmental Science, 2020, 13, 4057-4086.	15.6	241
5	Ternary nonfullerene polymer solar cells with efficiency >13.7% by integrating the advantages of the materials and two binary cells. Energy and Environmental Science, 2018, 11, 2134-2141.	15.6	223
6	Graphene/polypyrrole intercalating nanocomposites as supercapacitors electrode. Electrochimica Acta, 2013, 112, 44-52.	2.6	220
7	MnO2 Nanorods Intercalating Graphene Oxide/Polyaniline Ternary Composites for Robust High-Performance Supercapacitors. Scientific Reports, 2014, 4, 4824.	1.6	215
8	Recent development of the inverted configuration organic solar cells. Solar Energy Materials and Solar Cells, 2011, 95, 1785-1799.	3.0	210
9	Bacterial Cellulose Nanofiber-Supported Polyaniline Nanocomposites with Flake-Shaped Morphology as Supercapacitor Electrodes. Journal of Physical Chemistry C, 2012, 116, 13013-13019.	1.5	208
10	Highly efficient ternary polymer solar cells by optimizing photon harvesting and charge carrier transport. Nano Energy, 2016, 22, 241-254.	8.2	196
11	Efficient Ternary Polymer Solar Cells with Two Wellâ€Compatible Donors and One Ultranarrow Bandgap Nonfullerene Acceptor. Advanced Energy Materials, 2018, 8, 1702854.	10.2	195
12	A universal layer-by-layer solution-processing approach for efficient non-fullerene organic solar cells. Energy and Environmental Science, 2019, 12, 384-395.	15.6	193
13	Core–sheath structured bacterial cellulose/polypyrrole nanocomposites with excellent conductivity as supercapacitors. Journal of Materials Chemistry A, 2013, 1, 578-584.	5.2	175
14	Nematic liquid crystal materials as a morphology regulator for ternary small molecule solar cells with power conversion efficiency exceeding 10%. Journal of Materials Chemistry A, 2017, 5, 3589-3598.	5.2	173
15	Facile synthesis of mono-6-amino-6-deoxy-α-, β-, γ-cyclodextrin hydrochlorides for molecular recognition, chiral separation and drug delivery. Nature Protocols, 2008, 3, 691-697.	5.5	169
16	Three-Dimensional, Chemically Bonded Polypyrrole/Bacterial Cellulose/Graphene Composites for High-Performance Supercapacitors. Chemistry of Materials, 2015, 27, 7034-7041.	3.2	153
17	Biotemplated preparation of CdS nanoparticles/bacterial cellulose hybrid nanofibers for photocatalysis application. Journal of Hazardous Materials, 2011, 189, 377-383.	6.5	145
18	A multi-objective optimization-based layer-by-layer blade-coating approach for organic solar cells: rational control of vertical stratification for high performance. Energy and Environmental Science, 2019, 12, 3118-3132.	15.6	142

#	Article	IF	CITATIONS
19	The influence of fermentation conditions and post-treatment methods on porosity of bacterial cellulose membrane. World Journal of Microbiology and Biotechnology, 2010, 26, 125-131.	1.7	130
20	Stable and efficient CdS/Sb2Se3 solar cells prepared by scalable close space sublimation. Nano Energy, 2018, 49, 346-353.	8.2	130
21	Molecular engineering of central fused-ring cores of non-fullerene acceptors for high-efficiency organic solar cells. Journal of Materials Chemistry A, 2019, 7, 4313-4333.	5.2	122
22	Conformation Locking on Fusedâ€Ring Electron Acceptor for Highâ€Performance Nonfullerene Organic Solar Cells. Advanced Functional Materials, 2018, 28, 1705095.	7.8	120
23	Surface ligands engineering of semiconductor quantum dots for chemosensory and biological applications. Materials Today, 2017, 20, 360-376.	8.3	118
24	Simultaneous Improvement in Short Circuit Current, Open Circuit Voltage, and Fill Factor of Polymer Solar Cells through Ternary Strategy. ACS Applied Materials & Interfaces, 2015, 7, 3691-3698.	4.0	114
25	Dithieno[3,2â€b:2′,3′â€d]pyrrolâ€Cored Hole Transport Material Enabling Over 21% Efficiency Dopantâ€Fr Perovskite Solar Cells. Advanced Functional Materials, 2019, 29, 1904300.	ree 7.8	114
26	Sandwich-structured MnO ₂ /polypyrrole/reduced graphene oxide hybrid composites for high-performance supercapacitors. RSC Advances, 2014, 4, 9898-9904.	1.7	113
27	Conjugated Copolymers Based on Fluoreneâ^'Thieno[3,2-b]thiophene for Light-Emitting Diodes and Photovoltaic Cells. Macromolecules, 2007, 40, 6164-6171.	2.2	108
28	Dithieno[3,2â€b:2′,3′â€d]pyrrole Cored pâ€Type Semiconductors Enabling 20 % Efficiency Dopantâ€F Solar Cells. Angewandte Chemie - International Edition, 2019, 58, 13717-13721.	ree Perov 7.2	vskite 108
29	Suppressing photo-oxidation of non-fullerene acceptors and their blends in organic solar cells by exploring material design and employing friendly stabilizers. Journal of Materials Chemistry A, 2019, 7, 25088-25101.	5.2	107
30	Recent advances in pharmaceutical separations with supercritical fluid chromatography using chiral stationary phases. TrAC - Trends in Analytical Chemistry, 2012, 37, 83-100.	5.8	104
31	Nonfullerene Acceptor for Organic Solar Cells with Chlorination on Dithieno[3,2- <i>b</i> :2′,3′- <i>d</i>]pyrrol Fused-Ring. ACS Energy Letters, 2019, 4, 763-770.	8.8	102
32	Influence of PC60BM or PC70BM as electron acceptor on the performance of polymer solar cells. Solar Energy Materials and Solar Cells, 2012, 97, 71-77.	3.0	95
33	Bacteria Cellulose Nanofibers Supported Palladium(0) Nanocomposite and Its Catalysis Evaluation in Heck Reaction. Industrial & Engineering Chemistry Research, 2012, 51, 5743-5748.	1.8	93
34	Facile synthesis of bacterial cellulose fibres covalently intercalated with graphene oxide by one-step cross-linking for robust supercapacitors. Journal of Materials Chemistry C, 2015, 3, 1011-1017.	2.7	93
35	Improved Efficiency of Bulk Heterojunction Polymer Solar Cells by Doping Low-Bandgap Small Molecules. ACS Applied Materials & Interfaces, 2014, 6, 6537-6544.	4.0	91
36	Layered assembly of NiMn-layered double hydroxide on graphene oxide for enhanced non-enzymatic sugars and hydrogen peroxide detection. Sensors and Actuators B: Chemical, 2018, 260, 408-417.	4.0	90

#	Article	IF	CITATIONS
37	One-step facile synthesis of a simple carbazole-cored hole transport material for high-performance perovskite solar cells. Nano Energy, 2017, 40, 163-169.	8.2	89
38	Growth of Ni Mn layered double hydroxide and polypyrrole on bacterial cellulose nanofibers for efficient supercapacitors. Electrochimica Acta, 2019, 295, 82-91.	2.6	89
39	Efficient organic ternary solar cells with the third component as energy acceptor. Nano Energy, 2016, 26, 180-191.	8.2	88
40	High performance one-for-all phototheranostics: NIR-II fluorescence imaging guided mitochondria-targeting phototherapy with a single-dose injection and 808Anm laser irradiation. Biomaterials, 2020, 231, 119671.	5.7	87
41	Recent development of cationic cyclodextrins for chiral separation. TrAC - Trends in Analytical Chemistry, 2015, 65, 22-29.	5.8	86
42	MOF-derived Co3O4 nanosheets rich in oxygen vacancies for efficient all-solid-state symmetric supercapacitors. Electrochimica Acta, 2019, 328, 135103.	2.6	86
43	Key issues and recent progress of high efficient organic light-emitting diodes. Journal of Photochemistry and Photobiology C: Photochemistry Reviews, 2013, 17, 69-104.	5.6	83
44	Dithienothiophene (DTT)-Based Dyes for Dye-Sensitized Solar Cells: Synthesis of 2,6-Dibromo-DTT. Journal of Organic Chemistry, 2011, 76, 4088-4093.	1.7	81
45	High performance non-fullerene polymer solar cells based on PTB7-Th as the electron donor with 10.42% efficiency. Journal of Materials Chemistry A, 2018, 6, 2549-2554.	5.2	73
46	Efficient small molecular ternary solar cells by synergistically optimized photon harvesting and phase separation. Journal of Materials Chemistry A, 2015, 3, 16653-16662.	5.2	72
47	Characterization of bacteriostatic sausage casing: A composite of bacterial cellulose embedded with É-polylysine. Food Science and Biotechnology, 2010, 19, 1479-1484.	1.2	70
48	9.7%-efficient Sb ₂ (S,Se) ₃ solar cells with a dithieno[3,2- <i>b</i> : 2′,3′- <i>d</i>]pyrrole-cored hole transporting material. Energy and Environmental Science, 2021, 14, 359-364.	15.6	70
49	Highâ€Efficiency Nonfullerene Organic Solar Cells with a Parallel Tandem Configuration. Advanced Materials, 2017, 29, 1702547.	11.1	68
50	Immobilizing haemoglobin on gold/graphene–chitosan nanocomposite as efficient hydrogen peroxide biosensor. Sensors and Actuators B: Chemical, 2014, 197, 164-171.	4.0	67
51	Tuning of the conformation of asymmetric nonfullerene acceptors for efficient organic solar cells. Journal of Materials Chemistry A, 2019, 7, 22279-22286.	5.2	67
52	Cyclodextrin capped CdTe quantum dots as versatile fluorescence sensors for nitrophenol isomers. Nanoscale, 2015, 7, 19540-19546.	2.8	66
53	Oxygen vacancy-engineered Fe ₂ O ₃ nanoarrays as free-standing electrodes for flexible asymmetric supercapacitors. Nanoscale, 2019, 11, 12477-12483.	2.8	64
54	Recent development of conjugated oligomers for high-efficiency bulk-heterojunction solar cells. Solar Energy Materials and Solar Cells, 2010, 94, 1963-1979.	3.0	62

#	Article	IF	CITATIONS
55	Synthesis of cationic single-isomer cyclodextrins for the chiral separation of amino acids and anionic pharmaceuticals. Nature Protocols, 2007, 2, 3195-3200.	5.5	60
56	High-performance alloy model-based ternary small molecule solar cells. Nano Energy, 2016, 30, 276-282.	8.2	60
57	Binary hole transport materials blending to linearly tune HOMO level for high efficiency and stable perovskite solar cells. Nano Energy, 2018, 51, 680-687.	8.2	59
58	Over 15.7% Efficiency of Ternary Organic Solar Cells by Employing Two Compatible Acceptors with Similar LUMO Levels. Small, 2020, 16, e2000441.	5.2	59
59	Monosubstituted positively charged cyclodextrins: Synthesis and applications in chiral separation. Journal of Separation Science, 2008, 31, 3246-3256.	1.3	57
60	Retarding the Crystallization of a Nonfullerene Electron Acceptor for Highâ€Performance Polymer Solar Cells. Advanced Functional Materials, 2019, 29, 1807662.	7.8	57
61	Molecular Orientation Unified Nonfullerene Acceptor Enabling 14% Efficiency As ast Organic Solar Cells. Advanced Functional Materials, 2019, 29, 1903269.	7.8	56
62	Synthesis and application of single-isomer 6-mono(alkylimidazolium)-β-cyclodextrins as chiral selectors in chiral capillary electrophoresis. Electrophoresis, 2005, 26, 3839-3848.	1.3	55
63	Metal–organic framework-templated synthesis of sulfur-doped core–sheath nanoarrays and nanoporous carbon for flexible all-solid-state asymmetric supercapacitors. Nanoscale, 2018, 10, 15454-15461.	2.8	55
64	Poly(dithieno[3,2-b:2',3'-d]pyrrole) twisting redox pendants enabling high current durability in all-organic proton battery. Energy Storage Materials, 2021, 36, 1-9.	9.5	54
65	Metal-organic frameworks governed well-aligned conducting polymer/bacterial cellulose membranes with high areal capacitance. Energy Storage Materials, 2019, 23, 594-601.	9.5	53
66	13.9% Efficiency Ternary Nonfullerene Organic Solar Cells Featuring Low-Structural Order. ACS Energy Letters, 2019, 4, 2378-2385.	8.8	51
67	Enhanced performance of polymer solar cells through sensitization by a narrow band gap polymer. Solar Energy Materials and Solar Cells, 2013, 118, 30-35.	3.0	49
68	Chiral separation of dansyl amino acids in capillary electrophoresis using mono-(3-methyl-imidazolium)-β-cyclodextrin chloride as selector. Journal of Separation Science, 2007, 30, 1343-1349.	1.3	48
69	Novel β-cyclodextrin chiral stationary phases with different length spacers for normal-phase high performance liquid chromatography enantioseparation. Journal of Chromatography A, 2011, 1218, 3496-3501.	1.8	47
70	TD-DFT benchmark for UV-visible spectra of fused-ring electron acceptors using global and range-separated hybrids. Physical Chemistry Chemical Physics, 2020, 22, 7864-7874.	1.3	47
71	Modification on the Indacenodithieno[3,2- <i>b</i>]thiophene Core to Achieve Higher Current and Reduced Energy Loss for Nonfullerene Solar Cells. Chemistry of Materials, 2020, 32, 1297-1307.	3.2	46
72	Synthesis of ammonium substituted β-cyclodextrins for enantioseparation of anionic analytes. Tetrahedron Letters, 2005, 46, 1747-1749.	0.7	45

#	Article	IF	CITATIONS
73	Synthesis, characterization, and photovoltaic properties of novel conjugated copolymers derived from phenothiazines. Journal of Polymer Science Part A, 2007, 45, 5266-5276.	2.5	45
74	Efficient Bulk Heterojunction Solar Cells with Poly[2,7-(9,9-dihexylfluorene)-alt-bithiophene] and 6,6-Phenyl C61 Butyric Acid Methyl Ester Blends and Their Application in Tandem Cells. ACS Applied Materials & Interfaces, 2010, 2, 829-837.	4.0	45
75	Covalently intercalated graphene oxide for oil–water separation. Carbon, 2015, 82, 264-272.	5.4	45
76	Molecular engineering of acceptors to control aggregation for optimized nonfullerene solar cells. Journal of Materials Chemistry A, 2020, 8, 5458-5466.	5.2	45
77	Asymmetric simple unfused acceptor enabling over 12% efficiency organic solar cells. Chemical Engineering Journal, 2021, 412, 128770.	6.6	45
78	Hole Transport in Poly[2,7-(9,9-dihexylfluorene)-alt-bithiophene] and High-Efficiency Polymer Solar Cells from Its Blends with PCBM. ACS Applied Materials & Interfaces, 2009, 1, 1467-1473.	4.0	44
79	Crystallization behavior and mechanical properties of polypropylene random copolymer/poly(ethyleneâ€octene) blends. Journal of Applied Polymer Science, 2011, 122, 461-468.	1.3	44
80	Cationic cyclodextrin clicked chiral stationary phase for versatile enantioseparations in high-performance liquid chromatography. Journal of Chromatography A, 2016, 1467, 169-177.	1.8	44
81	Design of dopant-free small molecular hole transport materials for perovskite solar cells: a viewpoint from defect passivation. Journal of Materials Chemistry A, 2022, 10, 1150-1178.	5.2	44
82	Cationic cyclodextrin as versatile chiral selector for enantiomeric separation in capillary electrophoresis. Journal of Chromatography A, 2012, 1246, 98-102.	1.8	43
83	Novel cyclodextrin chiral stationary phases for high performance liquid chromatography enantioseparation: Effect of cyclodextrin type. Journal of Chromatography A, 2011, 1218, 5597-5601.	1.8	42
84	Cationic cyclodextrins chemically-bonded chiral stationary phases for high-performance liquid chromatography. Analytica Chimica Acta, 2012, 718, 121-129.	2.6	42
85	Juglone bonded carbon nanotubes interweaving cellulose nanofibers as self-standing membrane electrodes for flexible high energy supercapacitors. Chemical Engineering Journal, 2020, 396, 125325.	6.6	41
86	Effect of alkylimidazolium substituents on enantioseparation ability of single-isomer alkylimidazolium-β-cyclodextrin derivatives in capillary electrophoresis. Analytica Chimica Acta, 2007, 585, 227-233.	2.6	40
87	Cost-effective hole transporting material for stable and efficient perovskite solar cells with fill factors up to 82%. Journal of Materials Chemistry A, 2017, 5, 23319-23327.	5.2	40
88	2D Sideâ€Chain Engineered Asymmetric Acceptors Enabling Over 14% Efficiency and 75% Fill Factor Stable Organic Solar Cells. Advanced Functional Materials, 2020, 30, 2006141.	7.8	40
89	Transforming wood as nextâ€generation structural and functional materials for a sustainable future. EcoMat, 2022, 4, .	6.8	40
90	Improved permeability and selectivity in porous graphene for hydrogen purification. Physical Chemistry Chemical Physics, 2014, 16, 25755-25759.	1.3	39

#	Article	IF	CITATIONS
91	Evaluation of perphenylcarbamated cyclodextrin clicked chiral stationary phase for enantioseparations in reversed phase high performance liquid chromatography. Journal of Chromatography A, 2014, 1363, 119-127.	1.8	39
92	Boosting performance of inverted organic solar cells by using a planar coronene based electron-transporting layer. Nano Energy, 2017, 39, 454-460.	8.2	39
93	Manipulating Polymer Configuration to Accelerate Cation Intercalation Kinetics for Highâ€Performance Aqueous Zincâ€ŀon Batteries. Advanced Functional Materials, 2022, 32, .	7.8	38
94	Cyclodextrin clicked chiral stationary phases with functionalities-tuned enantioseparations in high performance liquid chromatography. Journal of Chromatography A, 2015, 1406, 342-346.	1.8	36
95	An unfused-ring acceptor with high side-chain economy enabling 11.17% as-cast organic solar cells. Materials Horizons, 2021, 8, 1008-1016.	6.4	36
96	Synthesis and application of mono-6-ammonium-6-deoxy-β-cyclodextrin chloride as chiral selector for capillary electrophoresis. Journal of Chromatography A, 2005, 1094, 187-191.	1.8	35
97	A family of single-isomer positively charged cyclodextrins as chiral selectors for capillary electrophoresis: Mono-6A-butylammonium-6A-deoxy-β-cyclodextrin tosylate. Electrophoresis, 2005, 26, 3125-3133.	1.3	35
98	A quinoxalinophenazinedione covalent triazine framework for boosted high-performance aqueous zinc-ion batteries. Journal of Materials Chemistry A, 2022, 10, 13868-13875.	5.2	35
99	Cyclodextrin-clicked silica/CdTe fluorescent nanoparticles for enantioselective recognition of amino acids. Nanoscale, 2016, 8, 5621-5626.	2.8	34
100	Synthesis of thieno[3,2-b]thiophene derived conjugated oligomers for field-effect transistors applications. Journal of Materials Chemistry, 2010, 20, 1497.	6.7	33
101	Bio-supported palladium nanoparticles as a phosphine-free catalyst for the Suzuki reaction in water. RSC Advances, 2012, 2, 1759.	1.7	33
102	Direct access to 4,8-functionalized benzo[1,2-b:4,5-b′]dithiophenes with deep low-lying HOMO levels and high mobilities. Journal of Materials Chemistry A, 2014, 2, 13580-13586.	5.2	33
103	Engineering Cyclodextrin Clicked Chiral Stationary Phase for High-Efficiency Enantiomer Separation. Scientific Reports, 2015, 5, 11523.	1.6	33
104	Enantioselective separation in capillary electrophoresis using a novel mono-6A-propylammonium-β-cyclodextrin as chiral selector. Analytica Chimica Acta, 2006, 555, 63-67.	2.6	32
105	Regulating the morphology of fluorinated non-fullerene acceptor and polymer donor via binary solvent mixture for high efficiency polymer solar cells. Science China Chemistry, 2019, 62, 1221-1229.	4.2	32
106	Hydroquinone versus Pyrocatechol Pendants Twisted Conjugated Polymer Cathodes for Highâ€Performance and Robust Aqueous Zincâ€Ion Batteries. Advanced Functional Materials, 2022, 32, 2108225.	7.8	32
107	A New Hole Transport Material for Efficient Perovskite Solar Cells With Reduced Device Cost. Solar Rrl, 2018, 2, 1700175.	3.1	31
108	The design of dithieno[3,2- <i>b</i> :2′,3′- <i>d</i>]pyrrole organic photovoltaic materials for high-efficiency organic/perovskite solar cells. Journal of Materials Chemistry A, 2020, 8, 22572-22592.	5.2	31

#	Article	IF	CITATIONS
109	High-temperature ferro-electricity in two-dimensional atomic crystal. Applied Physics Letters, 2013, 103, .	1.5	30
110	Over 15.5% efficiency organic solar cells with triple sidechain engineered ITIC. Science Bulletin, 2020, 65, 1533-1536.	4.3	30
111	Toughening and compatibilization of polyphenylene sulfide/nylon 66 blends with SEBS and maleic anhydride grafted SEBS triblock copolymers. Journal of Applied Polymer Science, 2007, 106, 2648-2655.	1.3	29
112	Facile synthesis of positively charged monosubstituted α- and γ-cyclodextrins for chiral resolution of anionic racemates. Tetrahedron: Asymmetry, 2007, 18, 1548-1553.	1.8	29
113	Synthesis, photophysics, theoretical modeling, and electroluminescence of novel 2,7â€carbazoleâ€based conjugated polymers with sterically hindered structures. Journal of Polymer Science Part A, 2008, 46, 7725-7738.	2.5	29
114	Hydroxyethylammonium monosubstituted cyclodextrin as chiral selector for capillary electrophoresis. Analytica Chimica Acta, 2013, 800, 95-102.	2.6	29
115	Tuning nanoscale morphology using mixed solvents and solvent vapor treatment for high performance polymer solar cells. RSC Advances, 2014, 4, 48724-48733.	1.7	29
116	A Cu ₃ PS ₄ nanoparticle hole selective layer for efficient inverted perovskite solar cells. Journal of Materials Chemistry A, 2019, 7, 4604-4610.	5.2	29
117	Chlorinated unfused acceptor enabling 13.57% efficiency and 73.39% fill factor organic solar cells via fine-tuning alkoxyl chains on benzene core. Chemical Engineering Journal, 2022, 427, 131828.	6.6	29
118	Enantioseparation of dansyl amino acids by a novel permanently positively charged single-isomer cyclodextrin: Mono-6-N-allylammonium-6-deoxy-β-cyclodextrin chloride by capillary electrophoresis. Analytica Chimica Acta, 2005, 546, 119-125.	2.6	28
119	Enantiomeric separation of 8 hydroxy, 10 carboxylic and 6 dansyl amino acids by mono(6-amino-6-deoxy)-β-cyclodextrin in capillary electrophoresis. Analytica Chimica Acta, 2005, 554, 156-162.	2.6	28
120	Methoxyethylammonium monosubstituted l²-cyclodextrin as the chiral selector for enantioseparation in capillary electrophoresis. Journal of Chromatography A, 2013, 1277, 84-92.	1.8	27
121	A Roomâ€Temperature Processable PDIâ€Based Electronâ€Transporting Layer for Enhanced Performance in PDIâ€Based Nonâ€Fullerene Solar Cells. Advanced Materials Interfaces, 2016, 3, 1600476.	1.9	27
122	Per(3-chloro-4-methyl)phenylcarbamate cyclodextrin clicked stationary phase for chiral separation in multiple modes high-performance liquid chromatography. Analytica Chimica Acta, 2016, 946, 96-103.	2.6	27
123	Nonacyclic carbazole-based non-fullerene acceptors enable over 12% efficiency with enhanced stability for organic solar cells. Journal of Materials Chemistry A, 2019, 7, 21903-21910.	5.2	26
124	Boosting PEDOT energy storage with redox dopant and electrolyte additive. Chemical Engineering Journal, 2020, 401, 126123.	6.6	26
125	Over 15% Efficiency in Ternary Organic Solar Cells by Enhanced Charge Transport and Reduced Energy Loss. ACS Applied Materials & Interfaces, 2020, 12, 21633-21640.	4.0	26
126	Enantioseparation of acidic enantiomers in capillary electrophoresis using a novel single-isomer of positively charged β-cyclodextrin: Mono-6A-N- pentylammonium-6A-deoxy-β-cyclodextrin chloride. Journal of Chromatography A, 2005, 1091, 152-157.	1.8	25

#	Article	IF	CITATIONS
127	Poly(vinylidene fluoride)/poly(methyl methacrylate)/TiO2 blown films: preparation and surface study. Journal of Materials Science, 2011, 46, 6656-6663.	1.7	25
128	A low temperature processable tin oxide interlayer via amine-modification for efficient and stable organic solar cells. Journal of Energy Chemistry, 2021, 56, 496-503.	7.1	25
129	Naphthodifuran alternating quinoxaline copolymers with a bandgap of â^1⁄41.2 eV and their photovoltaic characterization. New Journal of Chemistry, 2014, 38, 4816-4822.	1.4	24
130	Enhanced performance of polymer solar cells by employing a ternary cascade energy structure. Physical Chemistry Chemical Physics, 2014, 16, 16103-16109.	1.3	24
131	Earth-abundant nanotubes with layered assembly for battery-type supercapacitors. Chemical Engineering Journal, 2018, 350, 835-843.	6.6	24
132	Side chain engineering on dithieno[3,2- <i>b</i> :2,3- <i>d</i>]pyrrol fused electron acceptors for efficient organic solar cells. Materials Chemistry Frontiers, 2019, 3, 702-708.	3.2	24
133	Polyoxymethylene/thermoplastic polyurethane blends compatibilized with multifunctional chain extender. Journal of Applied Polymer Science, 2013, 127, 3033-3039.	1.3	23
134	Optimization of charge carrier transport balance for performance improvement of PDPP3T-based polymer solar cells prepared using a hot solution. Physical Chemistry Chemical Physics, 2015, 17, 9835-9840.	1.3	23
135	A dithieno[3,2-b:2′,3′-d]pyrrole-cored four-arm hole transporting material for over 19% efficiency dopant-free perovskite solar cells. Journal of Materials Chemistry C, 2019, 7, 9455-9459.	2.7	23
136	A Simple Dithieno[3,2â€b:2′,3′â€d]pyrrolâ€Rhodanine Molecular Third Component Enables Over 16.7% Efficiency and Stable Organic Solar Cells. Small, 2021, 17, e2007746.	5.2	22
137	Two-photon absorption, nonlinear optical and UV–vis spectral properties of 2-furanylmethyleneaminoantipyrine, benzylideneaminoantipyrine and cinnamilideneaminoantipyrine. Materials Chemistry and Physics, 2011, 129, 217-222.	2.0	21
138	Design and synthesis of triazoloquinoxaline polymers with positioning alkyl or alkoxyl chains for organic photovoltaics cells. Polymer Chemistry, 2014, 5, 1163-1172.	1.9	21
139	Heating induced aggregation in non-fullerene organic solar cells towards high performance. Journal of Energy Chemistry, 2021, 54, 131-137.	7.1	21
140	Processingâ€dependent high impact polystyrene/styreneâ€butadieneâ€styrene triâ€block copolymer/carbon black antistatic composites. Journal of Applied Polymer Science, 2012, 123, 1032-1039.	1.3	20
141	Interfacial layer for efficiency improvement of solution-processed small molecular solar cells. Solar Energy Materials and Solar Cells, 2013, 118, 135-140.	3.0	20
142	A family of singleâ€isomer, dicationic cyclodextrin chiral selectors for capillary electrophoresis: <scp>M</scp> onoâ€6 ^A â€ammoniumâ€6 ^C â€butylimidazoliumâ€î²â€cyclodextrin chlc Electrophoresis, 2013, 34, 833-840.	orides.	20
143	A versatile strategy to directly synthesize 4,8-functionalized benzo[1,2-b:4,5-bâ€2]difurans for organic electronics. Journal of Materials Chemistry A, 2015, 3, 1920-1924.	5.2	20
144	Effect of solvent additive and ethanol treatment on the performance of PIDTDTQx:PC71BM polymer solar cells. Solar Energy Materials and Solar Cells, 2015, 132, 528-534.	3.0	20

WEIHUA TANG

#	Article	IF	CITATIONS
145	A cationic cyclodextrin clicked bilayer chiral stationary phase for versatile chiral separation in HPLC. New Journal of Chemistry, 2018, 42, 3526-3533.	1.4	20
146	Carbonized wood-supported hollow NiCo2S4 eccentric spheres for high-performance hybrid supercapacitors. Journal of Alloys and Compounds, 2019, 811, 151858.	2.8	20
147	Enhancing phase separation with a conformation-locked nonfullerene acceptor for over 14.4% efficiency solar cells. Journal of Materials Chemistry C, 2019, 7, 13279-13286.	2.7	20
148	Synthesis and photovoltaic performance of novel thiophenyl-methylene-9H-fluorene-based low bandgap polymers. Polymer, 2013, 54, 4930-4939.	1.8	19
149	Two-Dimensional Polyfluorenes Bearing Thienylenevinylene π-Bridge-Acceptor Side Chains for Photovoltaic Solar Cells. Journal of Physical Chemistry C, 2013, 117, 24700-24709.	1.5	19
150	Correlation of structure and photovoltaic performance of benzo[1,2-b:4,5-b′]dithiophene copolymers alternating with different acceptors. New Journal of Chemistry, 2015, 39, 2248-2255.	1.4	19
151	Thiadiazole quinoxaline-based copolymers with â^¼1.0ÂeV bandgap for ternary polymer solar cells. Polymer, 2015, 79, 12-20.	1.8	19
152	The compatibilization effect of ethylene/styrene interpolymer on polystyrene/polyethylene blends. Journal of Polymer Science, Part B: Polymer Physics, 2007, 45, 2136-2146.	2.4	18
153	Efficiency improvement of polymer solar cells by iodine doping. Solid-State Electronics, 2011, 63, 83-83.	0.8	18
154	Side-chain Engineering of Benzo[1,2-b:4,5-b']dithiophene Core-structured Small Molecules for High-Performance Organic Solar Cells. Scientific Reports, 2016, 6, 25355.	1.6	18
155	13.76% efficiency nonfullerene solar cells enabled by selenophene integrated dithieno[3,2- <i>b</i> :2′,3′- <i>d</i>]pyrrole asymmetric acceptors. Materials Chemistry Frontiers, 2020, 4, 924-932.	3.2	18
156	Emerging polymer electrodes for aqueous energy storage. Materials Horizons, 2021, 8, 2373-2386.	6.4	18
157	High mobility acceptor as third component enabling high-performance large area and thick active layer ternary solar cells. Chemical Engineering Journal, 2021, 418, 129539.	6.6	18
158	Monosubstituted dually cationic cyclodextrins for stronger chiral recognition. RSC Advances, 2012, 2, 5088.	1.7	17
159	Evaluation of the chiral separation ability of singleâ€isomer cationic βâ€cyclodextrins in capillary electrophoresis. Electrophoresis, 2014, 35, 2744-2751.	1.3	17
160	Novel methoxypropylimmidazolium β-cyclodextrin for improved enantioseparation of amino acids. Talanta, 2014, 128, 460-465.	2.9	17
161	Triisopropylsilylethynyl substituted benzodithiophene copolymers: synthesis, properties and photovoltaic characterization. Journal of Materials Chemistry C, 2015, 3, 1595-1603.	2.7	17
162	Long lived photoexcitation dynamics in π-conjugated polymer and fullerene blended films. Organic Electronics, 2013, 14, 2058-2064.	1.4	16

#	Article	IF	CITATIONS
163	Enhanced performance of polymer solar cells by dipole-assisted hole extraction. Solar Energy Materials and Solar Cells, 2014, 130, 15-19.	3.0	16
164	Enantioseparation tuned by solvent polarity on a βâ€cyclodextrin clicked chiral stationary phase. Journal of Separation Science, 2015, 38, 3137-3144.	1.3	16
165	Design and photovoltaic characterization of dialkylthio benzo[1,2-b:4,5-b′]dithiophene polymers with different accepting units. Physical Chemistry Chemical Physics, 2015, 17, 7848-7856.	1.3	16
166	Selenium-substituted polymers for improved photovoltaic performance. Physical Chemistry Chemical Physics, 2016, 18, 7978-7986.	1.3	16
167	Hierarchical Nickel Sulfide Coated Halloysite Nanotubes For Efficient Energy Storage. Electrochimica Acta, 2017, 245, 51-58.	2.6	16
168	Dithieno[3,2â€b:2′,3′â€d]pyrrole Cored pâ€Type Semiconductors Enabling 20 % Efficiency Dopantâ€F Solar Cells. Angewandte Chemie, 2019, 131, 13855-13859.	ree Perov	skite 16
169	Exploration of a β-cyclodextrin clicked chiral stationary phase in high-performance liquid chromatography. Analytical Methods, 2014, 6, 2034-2037.	1.3	15
170	Synthesis and photovoltaic characterization of thiadiazole based low bandgap polymers. Thin Solid Films, 2014, 562, 75-83.	0.8	15
171	Methoxypropylamino β-cyclodextrin clicked AC regioisomer for enantioseparations in capillary electrophoresis. Analytica Chimica Acta, 2015, 868, 73-79.	2.6	15
172	Side-chain manipulation on accepting units of two-dimensional benzo[1,2- <i>b</i> :4,5- <i>b</i> ′]dithiophene polymers for organic photovoltaics. Polymer Chemistry, 2016, 7, 1486-1493.	1.9	15
173	Charge density modulation on asymmetric fused-ring acceptors for high-efficiency photovoltaic solar cells. Materials Chemistry Frontiers, 2020, 4, 1747-1755.	3.2	15
174	Asymmetric Reduction of Acetophenones with NaBH4 in the Presence of Mono-6-(1-methyl-3-imidazolium)-6-deoxy-β-cyclodextrin tosylate. Journal of Inclusion Phenomena and Macrocyclic Chemistry, 2006, 56, 287-290.	1.6	14
175	Carbazole‣ubstituted Triphenylamine and Diketopyrrolopyrrole Alternating Copolymer for Photovoltaic Cells. Macromolecular Chemistry and Physics, 2013, 214, 2136-2143.	1.1	14
176	Synthesis and Photovoltaic Performance of a [1,2,3]Triazolo[4,5â€g]quinoxalineâ€Based Lowâ€Bandgap Polymer. Macromolecular Chemistry and Physics, 2013, 214, 2473-2479.	1.1	14
177	Mono-6 ^A -(4-methoxybutylamino)-6 ^A -β-cyclodextrin as a chiral selector for enantiomeric separation. Journal of Separation Science, 2014, 37, 2056-2061.	1.3	14
178	Dicationic AC regioisomer cyclodextrins: mono-6A-ammonium-6C-alkylimidazolium-β-cyclodextrin chlorides as chiral selectors for enantioseparation. RSC Advances, 2012, 2, 12652.	1.7	13
179	Bacterial cellulose-assisted hydrothermal synthesis and catalytic performance of La2CuO4 nanofiber for methanol steam reforming. International Journal of Hydrogen Energy, 2013, 38, 10813-10818.	3.8	13
180	Graphene-Chitosan Composite Modified Electrode for Simultaneous Detection of Nitrophenol Isomers. Journal of the Electrochemical Society, 2015, 162, B269-B274.	1.3	13

#	Article	IF	CITATIONS
181	Bisalkylthio side chain manipulation on two-dimensional benzo[1,2- b :4,5- b ′]dithiophene copolymers with deep HOMO levels for efficient organic photovoltaics. Dyes and Pigments, 2017, 136, 312-320.	2.0	13
182	Hierarchical bimetallic hydroxide/chalcogenide core–sheath microarrays for freestanding ultrahigh rate supercapacitors. Nanoscale, 2020, 12, 72-78.	2.8	13
183	Robust graphene dispersion with amphiphlic perylene-polyglycidol. Materials Letters, 2014, 118, 188-191.	1.3	12
184	13.26% Efficiency Polymer Solar Cells by Optimizing Photogenerated Exciton Distribution and Phase Separation with the Third Component. Solar Rrl, 2019, 3, 1900269.	3.1	12
185	Efficient thick film non-fullerene organic solar cells enabled by using a strong temperature-dependent aggregative wide bandgap polymer. Chemical Engineering Journal, 2021, 405, 127033.	6.6	12
186	14.55% efficiency PBDB-T ternary organic solar cells enabled by two alloy-forming acceptors featuring distinct structural orders. Chemical Engineering Journal, 2021, 413, 127444.	6.6	12
187	Synergistic Interplay between Asymmetric Backbone Conformation, Molecular Aggregation, and Charge-Carrier Dynamics in Fused-Ring Electron Acceptor-Based Bulk Heterojunction Solar Cells. ACS Applied Materials & Interfaces, 2021, 13, 2961-2970.	4.0	12
188	Highly efficient organic solar cells enabled by a porous ZnO/PEIE electron transport layer with enhanced light trapping. Science China Materials, 2021, 64, 808-819.	3.5	12
189	Simple unfused acceptors with optimal naphthalene isomerization enabling 10.72% as-cast organic solar cells. Chemical Engineering Journal, 2022, 441, 135973.	6.6	12
190	Superâ€ŧoughed polymer blends derived from polypropylene random copolymer and ethylene/styrene interpolymer. Journal of Applied Polymer Science, 2010, 115, 190-197.	1.3	11
191	Hetero-nanostructure of silver nanoparticles on MO x (M = Mo, Ti and Si) and their applications. Science China Chemistry, 2011, 54, 865.	4.2	11
192	Synthesis and Photovoltaic Characterization of Dithieno[3,2â€b:2′,3′â€d]thiopheneâ€Đerived Narrowâ€Ba Polymers. Macromolecular Chemistry and Physics, 2014, 215, 227-234.	ndgap	11
193	Gold Nanoparticlesâ€Î²â€€yclodextrin hitosanâ€Graphene Modified Glassy Carbon Electrode for Ultrasensitive Detection of Dopamine and Uric Acid. Electroanalysis, 2014, 26, 2057-2064.	1.5	11
194	An asymmetric acceptor enabling 77.51% fill factor in organic solar cells. Science Bulletin, 2020, 65, 1876-1879.	4.3	11
195	Asymmetric small organic molecule-based NIR-II fluorophores for high performance tumor phototheranostics. Materials Chemistry Frontiers, 2021, 5, 5689-5697.	3.2	11
196	Porous Flexible Wood Scaffolds Designed for High-Performance Electrochemical Energy Storage. ACS Sustainable Chemistry and Engineering, 2022, 10, 7078-7090.	3.2	11
197	Luminescent and photovoltaic properties of poly(9,9-dioctylfluorene-co-bithiophene) in organic electronic devices. Science Bulletin, 2012, 57, 970-975.	1.7	10
198	Benzotrithiophene polymers with tuneable bandgap for photovoltaic applications. RSC Advances, 2014, 4, 53939-53945.	1.7	10

#	Article	IF	CITATIONS
199	Functionalities tuned enantioselectivity of phenylcarbamate cyclodextrin clicked chiral stationary phases in HPLC. Chirality, 2017, 29, 566-573.	1.3	10
200	Halloysite nanotubes favored facile deposition of nickel disulfide on NiMn oxides nanosheets for high-performance energy storage. Electrochimica Acta, 2018, 273, 349-357.	2.6	10
201	Unfused Acceptors Matching Ï€â€Bridge Blocks with Proper Frameworks Enable Over 12% Asâ€Cast Organic Solar Cells. Small, 2022, 18, .	5.2	10
202	Mechanical behaviors of ethylene/styrene interpolymer compatibilized polystyrene/polyethylene blends. Journal of Applied Polymer Science, 2007, 104, 4001-4007.	1.3	9
203	Simultaneous toughening of PPO/HIPS/Glass fiber reinforced composites with thermoplastic rubbers. Journal of Applied Polymer Science, 2014, 131, .	1.3	9
204	Pentacene nanostructural interlayer for the efficiency improvement of polymer solar cells. Thin Solid Films, 2011, 520, 676-679.	0.8	8
205	Doping a D-A structural polymer based on benzodithiophene and triazoloquinoxaline for efficiency improvement of ternary solar cells. Electronic Materials Letters, 2015, 11, 236-240.	1.0	8
206	Adjusting acceptor redistribution for highly efficient solvent additive-free polymer solar cells. Journal of Materials Chemistry C, 2016, 4, 3202-3208.	2.7	8
207	Acceptor manipulation of bisalkylthiothienyl benzo[1,2-b:4,5-b']dithiophene core-structured oligomers for efficient organic photovoltaics. Dyes and Pigments, 2017, 140, 512-519.	2.0	8
208	Low structure order acceptor as third component enables high-performance semitransparent organic solar cells. Chemical Engineering Journal, 2022, 428, 132640.	6.6	8
209	Carbonyl-enriched hierarchical carbon synergizes redox electrolyte for highly-efficient and stable supercapacitors. Chemical Communications, 2021, 57, 3716-3719.	2.2	8
210	Incorporating Perylene Moiety into Poly(phenothiazine-co-bithiophene) Backbone for Higher Charge Transport. Journal of Physical Chemistry B, 2008, 112, 3590-3596.	1.2	7
211	Synthesis, optical, electrochemical and electroluminescent properties of novel fluorene-alt-bithiophene copolymers bearing phenylvinyl bridged accepting side chains. European Polymer Journal, 2013, 49, 3610-3618.	2.6	7
212	Dialkylthio benzo[1,2-b:4,5-b′]difuran polymer for efficient organic photovoltaics with solvent treatment in active layers. Dyes and Pigments, 2016, 131, 356-363.	2.0	7
213	Exploring host–guest complexation mechanisms by a molecular dynamics/quantum mechanics/continuum solvent model approach. Chemical Physics Letters, 2016, 648, 170-177.	1.2	7
214	Enantioseparation of isoxazolines with functionalized perphenylcarbamate cyclodextrin clicked chiral stationary phases in HPLC. Electrophoresis, 2017, 38, 1939-1947.	1.3	7
215	Effect of bisalkylthio side chains on benzo[1,2- b :4,5- b â€2]dithiophene-based polymers for organic solar cells. Dyes and Pigments, 2017, 138, 47-55.	2.0	7
216	Intermolecular interaction induced spontaneous aggregation enables over 14% efficiency as-cast nonfullerene solar cells. Chemical Engineering Journal, 2022, 427, 131942.	6.6	7

#	Article	IF	CITATIONS
217	Catalyst-free nitro-coupling synthesis of azo-linked conjugated microporous polymers with superior aqueous energy storage capability. Science China Materials, 2022, 65, 958-966.	3.5	7
218	Preparation of High Quality Indium Tin Oxide Film on a Microbial Cellulose Membrane Using Radio Frequency Magnetron Sputtering. Chinese Journal of Chemical Engineering, 2011, 19, 179-184.	1.7	6
219	Photophysics and morphology of a polyfluorene donor–acceptor triblock copolymer for solar cells. Journal of Polymer Science, Part B: Polymer Physics, 2013, 51, 1705-1718.	2.4	6
220	A donor–acceptor liganded metal–organic framework showcases the hydrogen-bond-enhanced sensing of N-heterocyclic explosives. Journal of Materials Chemistry C, 2021, 9, 12086-12093.	2.7	6
221	Synthesis of sterically hindered antipyrines for intramolecularcharge transfer facilitated sensing. Journal of Physical Organic Chemistry, 2012, 25, 1112-1118.	0.9	5
222	Clicked AC regioisomer cationic cyclodextrins for enantioseparation. RSC Advances, 2014, 4, 54512-54516.	1.7	5
223	Evaluating the nature of the vertical excited states of fused-ring electron acceptors using TD-DFT and density-based charge transfer. Physical Chemistry Chemical Physics, 2021, 23, 15282-15291.	1.3	5
224	An unfused-ring acceptor enabling â^1⁄412% efficiency for layer-by-layer organic solar cells. Journal of Materials Chemistry C, 2022, 10, 10511-10518.	2.7	5
225	Noise characterization of light-emitting devices based on conjugated copolymers of fluorene and thiophene moieties. Journal of Applied Physics, 2007, 102, 063103.	1.1	4
226	The effect of metal electron cloud on the luminescence characteristics of organic ligands: An experimental and theoretical investigation. Science Bulletin, 2011, 56, 479-483.	1.7	4
227	Design and photovoltaic characterization of dithieno[3,2-b:2′,3′-d]silole copolymers with positioning phenyl groups. Physical Chemistry Chemical Physics, 2014, 16, 26893-26900.	1.3	4
228	Effect of carbon hybridization in 9H-fluorene unit on the photovoltaic properties of different fluorene-based conjugated polymers. High Performance Polymers, 2018, 30, 677-687.	0.8	4
229	Preparation and Characterization of Bacterial Cellulose Tube. , 2009, , .		3
230	Functional Cyclodextrin-Clicked Chiral Stationary Phases for Versatile Enantioseparations by HPLC. Methods in Molecular Biology, 2019, 1985, 147-157.	0.4	2
231	Modification of Cyclodextrin. , 2013, , 1-25.		1
232	Two-dimensional narrow bandgap conjugated polymers for high-efficiency solar cells. , 2011, , .		0
233	Cyclodextrin-Based Chiral Stationary Phases for High-Performance Liquid Chromatography. , 2013, , 67-101.		0
234	Cyclodextrin-Based Chiral Stationary Phases for Supercritical Fluid Chromatography. , 2013, , 103-143.		0

#	Article	IF	CITATIONS
235	Cationic Cyclodextrins for Capillary Electrophoresis. , 2013, , 225-258.		0
236	Perfluorosulfonated ionomers membranes: Meltâ€processing and characterization for ion exchange applications. Journal of Applied Polymer Science, 2014, 131, .	1.3	0